Extra Adenosine Stacks into the Self-Complementary d(CGCAGAATTCGCG) Duplex in Solution†

Dinshaw J. Patel,* Sharon A. Kozlowski, Luis A. Marky, Janet A. Rice, Chris Broka, Keiichi Itakura, and Kenneth J. Breslauer

ABSTRACT: The structural and energetic parameters for the helix to coil transition of the duplex formed by the self-complementary d($C_1G_2C_3AG_4A_5A_6T_6T_5C_4G_3C_2G_1$) sequence (henceforth called 13-mer duplex) that contains an extra noncomplementary dA residue between positions dC_3 and dG_4 are compared with the duplex formed by the corresponding self-complementary d(CGCGAATTCGCG) sequence (henceforth called 12-mer duplex) that lacks the extra base [Patel, D. J., Kozlowski, S. A., Marky, L. A., Broka, C., Rice, J. A., Itakuru, K., & Breslauer, K. J. (1981) *Biochemistry* (first paper of four in this issue)]. The nonexchangeable base proton nuclear magnetic resonance (NMR) resonances from the extra dA residue are identified and monitored through the melting transition of the 13-mer duplex. These markers demonstrate that the adenosine stacks into the 13-mer duplex rather than form a bulge loop. Furthermore, the base pairing on either side of the extra stacked dA residue remains intact. A downfield-shifted phosphorus resonance in the ^{31}P spectrum of the 13-mer duplex is tentatively assigned to the extended phosphodiester linkage opposite the stacked, extra dA residue. The nonexchangeable protons from base pairs 2–6 and the extra dA residue exhibit a duplex to strand transition midpoint of 57 ± 2 °C in 0.1 M phosphate solution. The thermally induced transition of the 13-mer duplex was also monitored by differential scanning calorimetry. This technique reveals that insertion of an extra dA into each strand of the duplex results in a 19 °C reduction in the melting temperature of the 13-mer relative to the 12-mer duplex. A calorimetric enthalpy change of 104 kcal (mol of double strand)$^{-1}$ and a van't Hoff enthalpy change of 70 kcal were determined for the helix to coil transition of the 13-mer duplex in 0.1 M NaCl solution. Comparison of these enthalpies reveals that the transition is not a two-state process and that the size of the cooperative unit is 9 ± 1 base pairs. The similarity between the calorimetric transition enthalpies for the 12-mer and 13-mer duplexes is consistent with a picture in which the stacking of the extra dA residue into the duplex on one strand compensates for the loss of stacking between dG·dC base pairs 3 and 4 at the site of the helix interruption.

There has been considerable effort to understand the structural role of noncomplementary base–base interactions in the interior of oligonucleotide and polynucleotide duplexes (Uhlenbeck et al., 1971; Martin et al., 1971; Gillam et al., 1975; Kallenbach et al., 1976; Topal & Fresco, 1976; Dodgson & Wells, 1977a, Early et al., 1978; Young & Kallenbach, 1978; Wallace et al., 1979; Cornelis et al., 1979; Haasnoot et al., 1980). These studies demonstrated that single dG·dA, dG·dG (Dodgson & Wells, 1977a), and dA·dC (Wallace et al., 1979) mismatches in the interior of duplexes reduce the helix stability by the equivalent of 3–4 base pairs. These single mismatches were resistant to single strand specific nucleases (Dodgson & Wells, 1977b) and did not interrupt the cooperative melting of duplex regions flanking the mismatch site. Both these observations suggest that the mismatch base pair is incorporated into the stacked duplex structure (Dodgson & Wells, 1977a; Wallace et al., 1979).

By contrast, there is limited information on the structure and energetics of helix interruptions containing an additional base on only one strand of the duplex (Fresco & Alberts, 1960; Seidel, 1966; Fink & Crothers, 1972; Lee & Tinoco, 1978). To increase our knowledge of such systems, we have carried out a nuclear magnetic resonance (NMR) and calorimetric investigation of the duplex formed by the self-complementary d(CGCAGAATTCGCG) sequence in which an internal adenosine lacks a hydrogen-bonding complement on the partner strand (Chart I).

Chart I

```
      CGCAGAATTC-GCG
      123  456654  321
      GCG-CTTAAGACGC
```

In this paper, proton and phosphorus NMR parameters of the 12-mer duplex d(CGCGAATTCGCG) and the 13-mer duplex d(CGCAGAATTCGCG) are used to determine whether the extra dA between base pairs 3 and 4 in the 13-mer duplex loops out into solution or stacks into the helix. The ability of NMR spectroscopy to monitor individual base pairs in oligonucleotide duplexes (Patel, 1974; Borer et al., 1975; Kallenbach et al., 1976; Early et al., 1977) permits an evaluation of the extent of localization of the structural change associated with the extra dA residues in the 13-mer duplex.

Differential scanning calorimetry provides a complete thermodynamic profile of thermally induced order–disorder transitions in RNA and DNA duplexes (Breslauer et al., 1975; Breslauer & Sturtevant, 1977; Albergo et al., 1981; Marky et al., 1981). Comparison of the calorimetric results on the 12-mer and 13-mer duplexes allows us to define the energetic consequences of the extra dA induced structural perturbations in the self-complementary 13-mer duplex. The nature of the transition is defined by comparing the model-independent calorimetric enthalpy with the derived model-dependent van't Hoff enthalpy.

† From Bell Laboratories, Inc., Murray Hill, New Jersey 07974 (D.J.P., S.A.K., and J.A.R.), the City of Hope National Medical Center, Duarte, California 91010 (C.B. and K.I.), and the Department of Chemistry, Douglass College, Rutgers University, New Brunswick, New Jersey 08903 (L.A.M. and K.J.B.). *Received April 28, 1981; revised manuscipt received September 3, 1981.* K.J.B. and L.A.M. gratefully acknowledge support from the National Institutes of Health, Grant GM-23509, the Research Corporation, and the Charles and Johanna Busch Memorial Fund.

0006-2960/82/0421-0445$01.25/0 © 1982 American Chemical Society

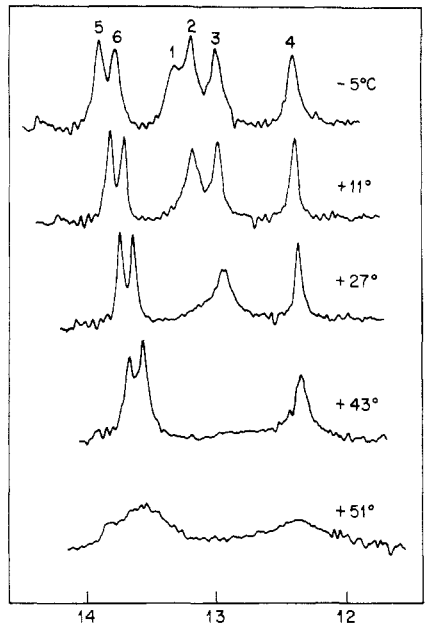

FIGURE 1: The temperature dependence of the 360-MHz correlation proton NMR spectra (12–14.5 ppm) of the 13-mer duplex in 0.1 M phosphate, 2.5 mM EDTA, and 4:1 $H_2O/^2H_2O$, pH 7.40, between −5 and +51 °C. The signal to noise of the spectra was improved by applying a 5-Hz exponential line broadening contribution. The assignment of individual imino protons to specific base pairs in the 13-mer sequence are designated above the resonances.

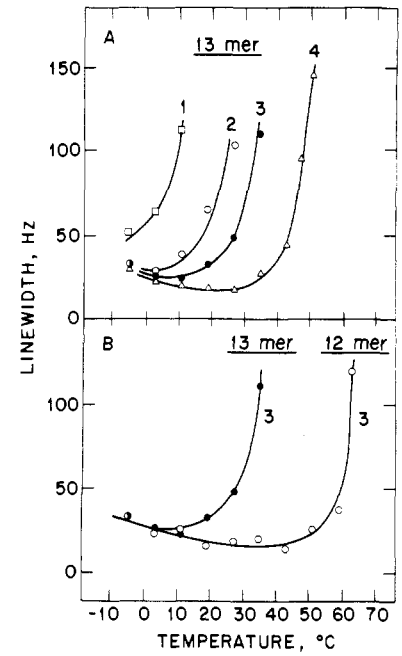

FIGURE 2: (A) The temperature dependence of the line widths of the four dG·dC imino protons of the 13-mer duplex in 0.1 M phosphate, 2.5 mM EDTA, and 4:1 $H_2O/^2H_2O$ at pH 7.40. (B) The temperature dependence of the line widths of the imino proton of dG·dC base pair 3 in the 13-mer duplex (●) and the 12-mer duplex (○) in 0.1 M phosphate, 2.5 mM EDTA, and 4:1 $H_2O/^2H_2O$ at pH 7.50 and 7.40, respectively.

Experimental Procedures

Synthesis. The d(CGCAGAATTCGCG) 13-mer was prepared by the modified triester method (Hirose et al., 1978) by coupling the protected tetramer DM–CGCA–PO^- with the protected nonamer HO–GAATTCGCG–OBz (Patel et al., 1981a) as described below.

The protected tetramer was synthesized by coupling 0.375 g of DM–CGC–PO^- (0.2 mmol) with 0.082 g of HO–A–PCE (0.14 mmol) in the presence of 0.3 mmol of TPSTe condensing agent. Workup and silica gel chromatography yielded DM–CGCA–PCE in 78% yield.

DM–CGCA–PCE (0.265 g, 0.11 mmol) was deblocked at its 3′ end and coupled with 0.3 g of HO–GAATTCGCG–OBz (0.07 mmol) in the presence of 0.25 mmol of TPSTe condensing agent. The protected 13-mer was chromatographed on silica gel, and the blocking groups were removed by treatment with base and acid as described previously (Patel et al., 1981a).

Chromatography of 2900 OD[1] units of the deblocked 13-mer on a DE-23 ion-exchange column yielded 300 OD units of pure d(CGCAGAATTCGCG), which was used for the NMR and calorimetric experiments.

NMR Spectra. The 13-mer exchangeable imino proton NMR spectra in H_2O, nonexchangeable proton NMR spectra in ^2H_2O, and phosphorus NMR spectra were recorded on the spectrometers described previously (Patel et al., 1981a). The phosphorus T_1 and nuclear Overhauser effect (NOE) experiments were undertaken as described previously (Patel et al., 1981a).

Calorimetry. The differential scanning calorimetry was carried out on a Microcal-1 instrument similar to one that has previously been described in detail (Jackson & Brandts, 1970). The experimental data are obtained as excess heat capacity vs. temperature. The concentration of the 13-mer was calculated with an extinction coefficient of 1.23×10^5 M^{-1} in strands at 25 °C (Cantor & Warshaw, 1970).

[1] Abbreviations: OD, optical density; EDTA, ethylenediaminetetraacetic acid.

Results

NMR Studies. We compare the NMR parameters for the 12-mer and the 13-mer duplexes at the Watson–Crick imino protons (monitor hydrogen bonding), the nonexchangeable base protons (monitor stacking interactions), and the backbone phosphates (monitor the O–P phosphodiester torsion and/or O–P–O bond angles) as a function of temperature.

(A) Imino Proton Line Widths. The 360-MHz proton correlation NMR spectrum (12–14 ppm) of the 13-mer duplex in 0.1 M phosphate and H_2O, pH 7.5, at −5 °C is presented in Figure 1. We observe six imino proton resonances in the 13-mer duplex corresponding to the six base pairs related by 2-fold symmetry, which demonstrates base pair formation along the entire length of the helix.

Studies on DNA fragments (Patel & Tonelli, 1974; Hilbers, 1979) and transfer RNA (Kearns et al., 1971; Schimmel & Redfield, 1980) suggest that the two imino resonances at lower field (13.75–13.95 ppm) correspond to the thymidine H-3 protons of dA·dT base pairs while the remaining four imino resonances at higher field (12.3–13.4 ppm) correspond to the four guanosine H-1 protons of dG·dC base pairs in the −5 °C spectra of the 13-mer duplex (Figure 1).

We observe a sequential broadening of three guanosine H-1 imino protons of the 13-mer duplex in 0.1 M phosphate, pH 7.4, on raising the temperature from −5 to +43 °C with the remaining guanosine H-1 and two thymidine H-3 imino protons broadening out above 50 °C (Figure 2). This sequential broadening (see Figures 1 and 2A) permits the assignment of the guanosine H-1 imino protons at 13.32, 13.19, 13.00, and 12.39 ppm to dG·dC base pairs 1, 2, 3, and 4, respectively (Table I).

We compare the line widths of the imino protons of dG·dC base pair 3 for the 12-mer duplex and the 13-mer duplex in 0.1 M phosphate, pH ~7.4 (Figure 2B). It is apparent that the imino proton of base pair 3 (Figure 2B) as well as other

Table I: Chemical Shifts of the Watson–Crick Imino Exchangeable Protons of the 12-mer Duplex[a] and the 13-mer Duplex[b] in 0.1 M Phosphate and 2.5 mM EDTA Solution

resonance[c]	assignment	chemical shifts at −5 °C (ppm) 12-mer	13-mer	Δ ppm
G(H-1)	1	13.29	13.32	−0.03
G(H-1)	2	13.14	13.19	−0.05
G(H-1)	3	12.96	13.00	−0.04
G(H-1)	4	12.74	12.39	0.35
T(H-3)	5	13.97	13.90	0.07
T(H-3)	6	13.86	13.78	0.08

[a] pH 7.50 (Patel et al., 1981a). [b] pH 7.40. [c] Guanosine H-1 assignments are based on the sequential broadening of the 12-mer and 13-mer imino exchangeable resonances with increasing temperature. The thymidine H-3 assignments are based on the sequential broadening of the d(GGAATTCC) duplex imino exchangeable resonances with increasing temperature.

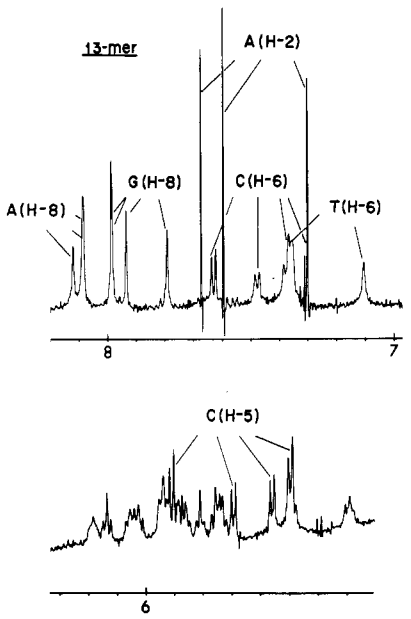

FIGURE 3: The 500-MHz Fourier transform proton NMR spectra (5.2–8.2 ppm) of the 13-mer duplex in 0.1 M phosphate, 2.5 mM EDTA, and ^2H_2O, pH 7.55, at ambient temperature. The resolution of the spectrum was improved by applying an exponential line narrowing contribution.

nonterminal base pairs in the 13-mer duplex broaden out below the corresponding imino protons in the 12-mer duplex, reflecting a decreased stability due to the mismatched dA residue between base pairs 3 and 4.

(*B*) *Imino Proton Chemical Shifts.* The chemical shifts of the six imino protons in the 12-mer duplex (Patel et al., 1981a) and the 13-mer duplex in 0.1 M phosphate at −5 °C are summarized in Table I. The guanosine H-1 imino proton of dG·dC base pair 4 shifts 0.35 ppm to high field on introduction of the mismatched dA between base pairs 3 and 4 while the remaining imino protons differ by <0.1 ppm between the two duplexes (Figure 1, Table I).

The thymidine H-3 imino protons of dA·dT base pairs 5 and 6 in the 13-mer duplex exhibit large temperature-dependent chemical shifts compared to the guanosine H-1 imino protons of dG·dC base pairs 2–4 (Figure 1). This demonstrates a premelting structural transition at the central dA·dT tetranucleotide core of the 13-mer duplex as was also observed for the 12-mer duplex (Patel et al., 1981a).

(*C*) *Nonexchangeable Proton Spectra.* The 500-MHz proton NMR spectra of the base-proton region (5.2–8.2 ppm) for the 13-mer duplex in 0.1 M phosphate at ambient temperature are presented in Figure 3. We have been able to assign many of the resonances to specific base pairs in the 13-mer duplex on the basis of decoupling, nuclear Overhauser effect, and chemical modification studies on a series of related self-complementary duplexes (Patel et al., 1981a).

Table II: Chemical Shift Parameters at the dA·dT Base Pairs for the 13-mer Duplex in 0.1 M Phosphate Solution

resonance	assignment[a]	ppm[b]	T_m (°C)
A(H-8)		8.08	56.0
A(H-8)		8.08	
A(H-2)	5	7.32	55.0
A(H-2)	6	7.68	57.5
T(H-6)	6	7.08	55.5
T(H-6)	5	7.35	55.5
$T(CH_3$-5)	6		
$T(CH_3$-5)	5	1.525	54.5

[a] Specific base pair assignments are based on chemical modifications and nuclear Overhauser effect measurements on the 12-mer and related analogues. [b] Duplex state at 30 °C.

Table III: Chemical Shift Parameters at the dG·dC Base Pairs for the 13-mer Duplex in 0.1 M Phosphate Solution

resonance	assignment[a]	ppm[b]	T_m (°C)
G(H-8)		7.78	
G(H-8)		7.94	
G(H-8)		7.97	
G(H-8)		8.10	
C(H-6)	2,3	7.36	60.0
C(H-6)	2,3	7.36	55.5
C(H-6)	4	7.47	54.0
C(H-6)	1	7.64	
C(H-5)	2,3	5.51	56.0
C(H-5)	2,3	5.56	57.0
C(H-5)	4	5.71	59.0
C(H-5)	1	5.97	

[a] Specific resonance assignments are based on spin decoupling and comparison with chemical shifts of $(dC\text{-}dG)_3$ hexanucleotide duplex. [b] Duplex state at 30 °C.

The chemical shifts of the two dA·dT base pair protons in the 13-mer duplex at 30 °C (T_m = 57 °C) in 0.1 M phosphate are presented in Table II with the corresponding data for the four dG·dC base pair protons summarized in Table III. In addition, the corresponding transition midpoints at individual resonances of the 13-mer duplex in 0.1 M phosphate are listed in Tables II and III.

(*D*) *Extra dA Residue.* The d(CGCGAATTCGCG) 12-mer duplex and the d(CGCAGAATTCGCG) 13-mer duplex have a common d(GAATTC) hexanucleotide core containing symmetry-related base pairs 4–6. Thus, based purely on nearest-neighbor effects, we expect dA·dT base pairs 5 and 6 to have common conformational properties and NMR parameters in the two duplexes. Our strategy was to identify the extra adenosine in the 13-mer duplex by its distinct NMR parameters during the melting transition.

The three adenosine H-8 resonances are centered at about 8.1 ppm, and the three sharp adenosine H-2 resonances are observed between 7.2 and 7.7 ppm for the 13-mer duplex at ambient temperature (Figure 3). The temperature dependence through the melting transitions of the adenosine H-8 and H-2 chemical shifts for the 12-mer and 13-mer duplexes in 0.1 M phosphate are plotted in Figure 4. The H-8 and H-2 resonances from the extra adenosine in the 13-mer duplex can be readily identified on the basis of their unique chemical shift in the duplex and strand states (Figure 4).

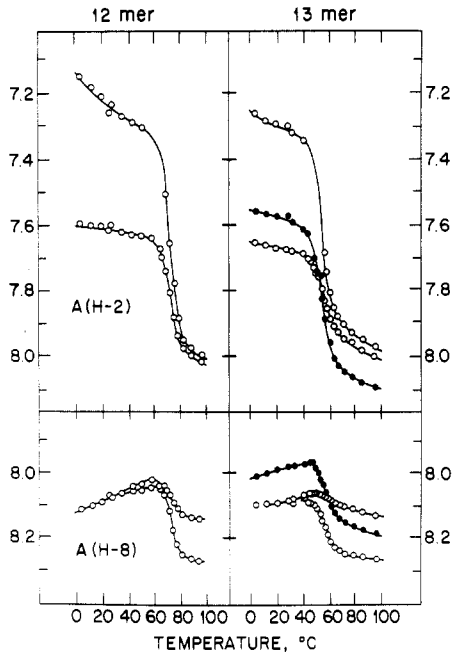

FIGURE 4: The temperature dependence of the adenosine H-8 and H-2 resonances in the 12-mer and the 13-mer duplexes in 0.1 M phosphate, 2.5 mM EDTA, and ^2H_2O. The adenosine resonances at positions 5 and 6 in the 12-mer and 13-mer duplexes are represented by (○) while the extra adenosine in the 13-mer duplex is represented by (●).

Table IV: Chemical Shift Parameters for the Extra Adenosine in the 13-mer Duplex in 0.1 M Phosphate Solution

resonance	chemical shift ppm[a]	chemical shift Δ ppm[b]	T_m (°C)
A(H-8)	7.97	0.21	57.5
A(H-2)	7.59	0.51	55.0

[a] Chemical shift in duplex state at 30 °C. [b] Chemical shift difference between 95 and 30 °C.

The NMR parameters for the extra adenosine residue during the melting transition of the 13-mer duplex are tabulated in Table IV. It is apparent that the 0.21-ppm adenosine H-8 and 0.51-ppm adenosine H-2 upfield shifts on duplex formation (Table IV) are comparable to the corresponding values for the adenosine residues at positions 5 and 6 (Figure 4). This result demonstrates that all three adenosines in the 13-mer sequence are stacked with adjacent base pairs in the duplex state.

(*E*) *Duplex to Strand Transition.* The nonexchangeable adenosine (Figure 4), thymidine, cytidine, and guanosine base protons shift as average resonances during the duplex to strand transition of the 13-mer duplex in aqueous solution. The transition midpoints can be evaluated from individual melting curves and are listed in Tables II–IV for the extra adenosine and nonterminal base pairs of the 13-mer duplex. The proton markers from base pairs 2–6 and the stacked adenosine exhibit a common duplex to strand transition midpoint of 57 ± 2 °C in 0.1 M phosphate solution. The chemical shift change associated with the melting of the terminal dG·dC base pair is quite small. Therefore, it is not possible to evaluate the T_m associated with the helix–coil transition at base pair 1 at either end of the 13-mer duplex.

We note that the transition midpoint of 72 ± 1 °C for the 12-mer duplex (Patel et al., 1981a) decreases to 57 ± 2 °C for the 13-mer duplex as measured by the nonexchangeable protons in 0.1 M phosphate solution. Thus, a 15 °C decrease in thermal stability for the duplex state is induced by the presence of the stacked, extra adenosine residues (Chart I).

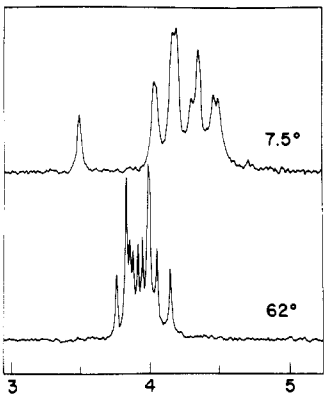

FIGURE 5: The proton noise decoupled 80.995-MHz Fourier transform phosphorus NMR spectra (3.0–5.0 ppm upfield from standard trimethyl phosphate) of the 13-mer duplex in 20 mM phosphate, 0.5 mM EDTA, and ^2H_2O, pH 8.2, at 7.5 and 62 °C. The chemical shifts are not corrected for the temperature dependence of the standard.

Table V: 81-MHz ^{31}P Spin–Lattice Relaxation Times (T_1) and Nuclear Overhauser Effect ($1 + \eta$) for the Resolved Phosphodiesters in the 13-mer Duplex at 20 °C[a]

chemical shift (ppm)[b]	area	relaxation time[c] T_1 (s)	NOE[c] $(1 + \eta)$
3.549	1	1.44	1.18
4.021	2	1.83	1.02
4.092[d]	1	1.86	1.06
4.143	3	1.79	1.09
4.252	1	1.83	1.01
4.304	2	1.76	1.05
4.434	2	1.58	1.05

[a] Buffer: 20 mM phosphate, 0.5 mM EDTA, and ^2H_2O, pH 8.2. [b] Upfield from internal standard trimethyl phosphate. [c] The repetition delay between pulses was 10 s. [d] Shoulder on 4.143-ppm resonance.

(*F*) *Phosphorus Chemical Shifts.* The proton noise decoupled 81-MHz ^{31}P spectrum of the 13-mer duplex in 20 mM phosphate and ^2H_2O, pH 8.2, at 7.5 °C is presented in Figure 5. We observe differences in the spectral dispersion between 4.0 and 4.5 ppm for the 13-mer (Figure 5) and 12-mer (Patel et al., 1981a) duplexes. The 13-mer duplex contains, in addition, one phosphodiester shifted downfield from the main cluster of resonances (Figure 5). This shifted resonance most likely arises from the phosphodiester at the helix interruption site in the 13-mer duplex and provides an additional marker for this type of perturbation in a regular duplex. During the thermally induced duplex to strand transition of the 13-mer, the phosphorus resonances in the main cluster shift downfield while the resolved phosphodiester at 3.48 ppm shifts upfield (Figure 5).

We observe small differences in the ^{31}P spin–lattice relaxation times (T_1) and $^{31}P[^1H]$ nuclear Overhauser effect ($1 + \eta$) value for the 3.55-ppm downfield-shifted phosphodiester resonances when compared to the remaining phosphodiester resonances in the main cluster between 4.0 and 4.5 ppm at 20 °C (Table V).

Calorimetric Studies. In Figure 6, the calorimetric heat capacity curves for the 12-mer (Patel et al., 1981a) and 13-mer duplexes in 0.1 M NaCl are compared. The transition midpoints are 71.3 °C for the 12-mer (Patel et al., 1981a) and 52.0 °C for the 13-mer duplex.

(*A*) *Calorimetric Enthalpy.* We obtain a transition enthalpy of 104 kcal (mol of double strand)$^{-1}$ for the 13-mer duplex by integration of the area under the heat capacity curve shown

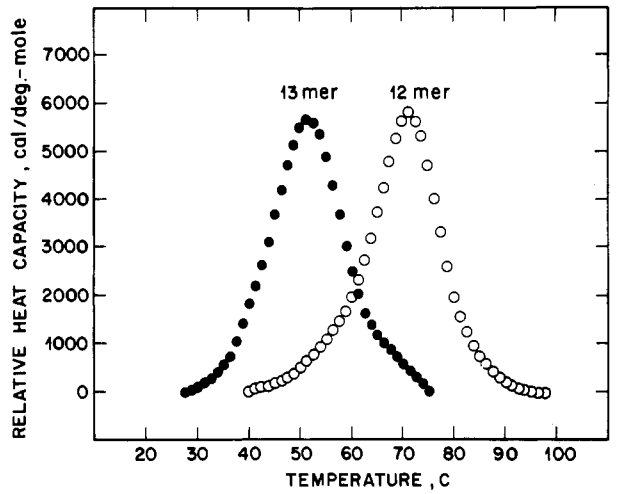

FIGURE 6: Calorimetric heat capacity vs. temperature curves for the 12-mer and the 13-mer duplexes in 0.1 M NaCl, 10 mM phosphate, and 0.1 mM EDTA, pH 7.0. The strand concentration is 0.696 mM. The temperature was scanned from 10 to 95 °C at a rate of ~1 °C/min.

Table VI: Calorimetric and van't Hoff Enthalpies for the Melting Transition of the 12-mer and the 13-mer Duplexes in 0.1 M NaCl Solution[a]

	ΔH_{cal} (kcal)	$\Delta H_{V.H.}$ (kcal)	T_m (°C)
12-mer[b]	102	74	71.3
13-mer	104	70	52.0

[a] Buffer: 0.1 M NaCl, 10 mM phosphate, and 0.1 mM EDTA, pH 7.0. Calorimetric data represent averages of at least three independent determinations. [b] Patel et al. (1981a).

in Figure 6. This transition enthalpy for the 13-mer duplex is essentially indistinguishable from the corresponding value of the 12-mer duplex (Patel et al., 1981a) (Table VI). Thus, incorporation of the extra adenosine residue between the third and fourth position from each end does not significantly alter the enthalpy of the duplex to strand transition despite the extra adenosine induced decrease of 19 °C in the melting temperature of the 13-mer duplex relative to the 12-mer duplex.

(B) van't Hoff Enthalpy. The van't Hoff enthalpy change can be analyzed from the shape of the calorimetric heat capacity curve as described previously (Gralla & Crothers, 1973; Patel et al., 1981a). Using this approach, we obtain a transition enthalpy of 70 kcal for the 13-mer duplex, which is of similar magnitude to that reported previously for the 12-mer duplex (Patel et al., 1981a) (Table VI). The 13-mer and 12-mer duplexes both exhibit model-dependent van't Hoff enthalpies that are substantially lower in magnitude than the model-independent calorimetric values (Table VI).

Discussion

Structural Aspects. We have been able to assign the proton resonances of individual base pairs in the 12-mer d-(CGCGAATTCGCG) (Patel et al., 1981a) and 13-mer d-(CGCAGAATTCGCG) duplexes at the exchangeable (Table I) and nonexchangeable (Tables II and III) protons. This permits a detailed evaluation of the structure and dynamics of the modification site and its immediate environment in the 13-mer duplex in solution.

Stacked Adenosine. The H-8 and H-2 protons of the extra adenosine undergo large upfield shifts on formation of the 13-mer duplex (Table IV, Figure 4). This unambiguously demonstrates stacking of the adenosine ring into the duplex with the ring currents (Giessner-Prettre et al., 1976; Arter & Schmidt, 1976) from dG·dC base pairs 3 and 4 shifting the adenosine base protons to high field.

Base Pairing Adjacent to Stacked Adenosine. We are able to observe the guanosine H-1 imino protons from positions 3 and 4 in the 13-mer spectrum at low temperature (Figure 1). This demonstrates Watson–Crick dG·dC base pair formation adjacent to the stacked adenosine residue. Thus, the insertion of an extra adenosine into the helix does not rupture the adjacent base pairing interactions.

Chemical shift differences between the 12-mer (Patel et al., 1981a) and 13-mer duplexes are observed at the guanosine H-1 resonance of base pair 4 (Figure 1, Table I), one guanosine H-8 resonance (Table III), and two nonterminal cytidine H-5 and H-6 (Table III) resonances. These differences reflect the base pair overlap changes at positions 3 and 4 on proceeding from the 12-mer to the 13-mer duplex. In the 12-mer, the two dG·dC base pairs stack with each other while in the 13-mer duplex the extra adenosine is inserted between these base pairs.

By contrast there are no significant chemical shift differences at the dA·dT base resonances at positions 5 and 6 between the 12-mer (Patel et al., 1981a) and 13-mer duplexes (Figure 4, Table II). This is reasonable since the mismatched adenosine is separated from the dA·dT tetranucleotide core by a dG·dC base pair.

Modification Site. We have demonstrated that the extra adenosine stacks between base pairs 3 and 4 in the 13-mer duplex in solution. This insertion requires that the two dG·dC base pairs be separated by greater than 3.4 Å at the modification site. This would result in a nonstandard phosphodiester linkage on the opposite strand, which lacks the complementary base. We tentatively assign the well-resolved, downfield-shifted phosphorus resonance at 3.48 ppm in the 13-mer duplex at 7.5 °C (Figure 5) to the extended $dC_4(3'–5')dG_3$ phosphodiester linkage on the partner strand opposite the mismatched dA residue. The downfield shift and altered phosphorus relaxation parameters (Table V) suggest that this phosphodiester linkage changes from the standard O–P–O bond and/or O–P torsion angles (Patel, 1976; Gorenstein et al., 1976). This provides an example of the potential of ^{31}P NMR to monitor conformational changes in the sugar–phosphate backbone of nucleic acid duplexes (Patel, 1974, 1979; Gueron & Shulman, 1975; Patel et al., 1979, 1981c; Davanloo et al., 1979; Salemink et al., 1981).

Melting Transition. The stacking of the extra adenosine could be visualized as a spacer between the hexanucleotide core (symmetry-related base pairs 4–6) and the trinucleotide segments (base pairs 1–3) at either end of the 13-mer duplex. It is of interest to determine whether the 13-mer duplex melts as a continuous helix or whether the central hexanucleotide domain melted at a different temperature than the trinucleotide ends. The three nonterminal dG·dC residues (Table III), the two dA·dT residues (Table II), and the extra adenosine (Table IV) exhibit a common transition midpoint of 57 ± 2 °C for the 13-mer duplex in 0.1 M phosphate solution. These results demonstrate that the 10 nonterminal base pairs of the 13-mer duplex melt as a cooperative unit.

Premelting Transition. The sequential broadening of the guanosine H-1 protons of the four dG·dC base pairs in the 13-mer duplex in 0.1 M phosphate, pH 7.40 (Figure 2A), demonstrate fraying at the ends of the duplex (Patel, 1974; Patel & Hilbers, 1975; Kan et al., 1975).

The imino protons of the central dA·dT base pairs exhibit large temperature-dependent chemical shifts (0.25 ppm between −5 and +43 °C), which are not observed at the imino protons of the three nonterminal dG·dC base pairs in the

13-mer duplex. The observed upfield shifts of the thymidine imino protons with increasing temperature could reflect variations in the extent of duplex unwinding and/or base pair propeller twisting at the dA·dT base pairs in the center of the duplex.

Overall Stability. A comparison of the transition midpoints (Table VI) derived from the heat capacity curves of the 12-mer and 13-mer duplexes (Figure 6) reveals that insertion of an extra adenosine residue causes a 19 °C destabilization of the oligonucleotide duplex.

Enthalpy Change. The calorimetric transition enthalpies of the 12-mer and 13-mer duplexes are essentially equal despite the destablization of the 13-mer relative to the corresponding 12-mer duplex. Since the NMR data reveal that the extra adenosine residue introduces only nearest-neighbor changes in base stacking in the 13-mer relative to the 12-mer, we can conclude that the structural perturbation is a local phenomenon. Thus, two possible explanations can be offered for the equal transition enthalpies observed for the 12-mer and 13-mer duplexes. The extra adenosine residue may bulge out and not significantly interfere with or disrupt the stacking interactions found in the 12-mer, thereby resulting in equal transition enthalpies. This picture is not supported by the NMR data. Alternatively, in conjunction with the NMR data, it can be suggested that the extra adenosine residue stacks into the helix. This extra stacking, however, may well be balanced by the stretching disruption of the dC_4 and dG_3 stacking on the partner strand at the position opposite the inserted extra dA residue. Thus, the equal transition enthalpies for the 12-mer and 13-mer duplexes may simply imply that the energetics for these two extra adenosine induced structural alterations have equal but opposite signs.

Implicit in the reasoning described above is a very reasonable assumption that the high-temperature, single-stranded states of the two oligomers are approximately isoenergetic. The high-temperature NMR data on the 12-mer and 13-mer duplexes (Figure 4) support this assumption.

The heat capacity curves exhibit the same pretransition and posttransition base lines (Figure 6) so that the change in heat capacity at constant pressure (ΔC_p) for the 12-mer and 13-mer transitions is close to zero. These conclusions parallel similar observations based on calorimetric studies of other deoxyoligonucleotides (Marky et al., 1981; Albergo et al., 1981).

Nature of the Transition. As described previously (Patel et al., 1981a), the transition occurs in a highly cooperative, two-state manner when $\Delta H_{cal} = \Delta H_{V.H.}$ while $\Delta H_{V.H.} < \Delta H_{cal}$ when intermediate states are significantly populated (Tsong et al., 1970).

The van't Hoff enthalpy (70 kcal) is considerably smaller than the calorimetrically determined value [104 kcal (mol double strand)$^{-1}$] for the 13-mer duplex in 0.1 M NaCl solution so that the helix–coil transition does not occur in an all-or-none manner but rather involves partial opening of the helix prior to the cooperative component of the transition. A similar conclusion was reached previously for the 12-mer duplex in 0.1 M NaCl solution (Patel et al., 1981a). From the ratio of the van't Hoff and calorimetric enthalpies, the size of the cooperative units are calculated to be about 70% of both duplex structures. Significantly, this cooperative length of 9 ± 1 base pairs remains unchanged despite the extra dA induced destabilization of the 13-mer duplex relative to the 12-mer duplex.

Finally, since the two duplexes have similar transition enthalpies but T_m values that differ by 19 °C, we suggest that the destabilization of the 13-mer relative to the 12-mer is entropic in origin. In this connection, it is quite possible that the geometric constraints at the modification site are quite severe (e.g., the unusually stretched $dC_4(3'–5')dG_3$ phosphodiester linkage), thereby lowering the entropy of the 13-mer relative to the 12-mer duplex. This would lead to a larger entropy change favoring disruption of the helix, which would be reflected by the observed lower melting temperature. The same note of caution described in the preceding paper (Patel et al., 1981b) concerning the limits of such an analysis of the data also applies to the interpretion of the 13-mer duplex data just presented.

Acknowledgments

The 360-MHz correlation spectra were recorded at the Mid Atlantic Regional Facility (funded by National Institutes of Health Grant RR542) and 500-MHz Fourier transform spectra were recorded at the Cal Tech Facility (funded by National Science Foundation Grant CHE-7916324). We thank T. Perkins and U. Banerjee for recording the 500-MHz spectrum.

References

Albergo, D., Marky, L., Breslauer, K., & Turner, D. (1981) *Biochemistry 20*, 1409–1413.

Arter, D. B., & Schmidt, P. G. (1976) *Nucleic Acids Res. 3*, 1437–1447.

Borer, P. N., Kan, L. S., & T'so, P. O. P. (1975) *Biochemistry 14*, 4847–4863.

Breslauer, K. J., & Sturtevant, J. M. (1977) *Biophys. Chem. 7*, 205–209.

Breslauer, K. J., Sturtevant, J. M., & Tinoco, I., Jr. (1975) *J. Mol. Biol. 99*, 549–565.

Cantor, C., & Warshaw, M. W. (1970) *Biopolymers 9*, 1059–1077.

Cornelis, A. G., Haasnoot, J. H. J., den Hartog, J. R., de Rooij, M., van Boom, J. H., & Altona, C. (1979) *Nature (London) 281*, 235–236.

Davanloo, P., Armitage, I. M., & Crothers, D. M. (1979) *Biopolymers 18*, 663–680.

Dodgson, J. B., & Wells, R. D. (1977a) *Biochemistry 16*, 2367–2374.

Dodgson, J. B., & Wells, R. D. (1977b) *Biochemistry 16*, 2374–2379.

Early, T. A., Kearns, D. R., Burd, J. F., Larson, J. E., & Wells, R. D. (1977) *Biochemistry 16*, 541–551.

Early, T. A., Olmsted, J., III, Kearns, D. R., & Lezius, A. G. (1978) *Nucleic Acids Res. 5*, 1955–1970.

Fink, T., & Crothers, D. M. (1972) *J. Mol. Biol. 66*, 1–12.

Fresco, J. R., & Alberts, B. M. (1960) *Proc. Natl. Acad. Sci. U.S.A. 46*, 311–321.

Giessner-Prettre, C., Pullman, B., Borer, P. N., Kan, L. S., & T'so, P. O. P. (1976) *Biopolymers 15*, 2277–2286.

Gillam, S., Waterman, K., & Smith, M. (1975) *Nucleic Acids Res. 2*, 625–634.

Gorenstein, D. G., Findlay, J. B., Momii, R. K., Luxon, B. A., & Kar, D. (1976) *Biochemistry 15*, 3796–3803.

Gralla, J., & Crothers, D. M. (1973) *J. Mol. Biol. 78*, 301–319.

Guêron, M., & Shulman, R. G. (1975) *Proc. Natl. Acad. Sci. U.S.A. 72*, 3482–3485.

Haasnoot, C. A. G., den Hartog, J. H. J., de Rooij, J. F. M., van Boom, J. H., & Altona, C. (1980) *Nucleic Acids Res. 8*, 169–181.

Hilbers, C. W. (1979) in *Biological Applications of Magnetic Resonance* (Shulman, R. G., Ed.) pp 1–43, Academic Press, New York.

Hirose, T., Crea, R., & Itakura, K. (1978) *Tetrahedron Lett. 28*, 2449-2452.
Jackson, W. M., & Brandts, J. F. (1970) *Biochemistry 9*, 2295-2301.
Kallenbach, N. R., Daniel, W. E., Jr., & Kaminker, M. A. (1976) *Biochemistry 15*, 1218-1224.
Kan, L. S., Borer, P. N., & T'so, P. O. P. (1975) *Biochemistry 14*, 4864-4869.
Kearns, D. R., Patel, D. J., & Shulman, R. G. (1971) *Nature (London) 229*, 338-339.
Lee, C. H., & Tinoco, I., Jr. (1978) *Nature (London) 274*, 609-610.
Marky, L. A., Canuel, L., Jones, R. A., & Breslauer, K. J. (1981) *Biophys. J. 13*, 141-149.
Martin, F. H., Uhlenbeck, O. C., & Doty, P. (1971) *J. Mol. Biol. 57*, 201-215.
Patel, D. J. (1974) *Biochemistry 13*, 2388-2395.
Patel, D. J. (1976) *Biopolymers 15*, 533-558.
Patel, D. J. (1979) *Eur. J. Biochem. 99*, 369-378.
Patel, D. J., & Tonelli, A. E. (1974) *Biopolymers 13*, 1943-1964.
Patel, D. J., & Hilbers, C. W. (1975) *Biochemistry 14*, 2651-2656.
Patel, D. J., Canuel, L. L., & Pohl, F. M. (1979) *Proc. Natl. Acad. Sci. U.S.A. 76*, 2508-2511.
Patel, D. J., Kozlowski, S. A., Marky, L. A., Broka, C., Rice, J. A., Itakura, K., & Breslauer, K. J. (1981a) *Biochemistry* (first paper of four in this issue).
Patel, D. J., Kozlowski, S. A., Marky, L. A., Rice, J. A., Broka, C., Dallas, J., Itakura, K., & Breslauer, K. J. (1981b) *Biochemistry* (second paper of four in this issue).
Patel, D. J., Kozlowski, S., Suggs, W., & Cox, S. (1981c) *Proc. Natl. Acad. Sci. U.S.A. 78*, 4063-4067.
Salemink, P. J. M., Raue, H. A., Heerschap, A., Planta, R. J., & Hilbers, C. W. (1981) *Biochemistry 20*, 265-272.
Schimmel, P. R., & Redfield, A. G. (1980) *Annu. Res. Biophys. Bioeng. 9*, 181-221.
Seidel, H. (1966) *Biochim. Biophys. Acta 129*, 412-414.
Topal, M. D., & Fresco, J. D. (1976) *Nature (London) 263*, 285-293.
Tsong, T. Y., Hearn, R. P., Wrathall, D. P., & Sturtevant, J. M. (1970) *Biochemistry 9*, 2666-2677.
Uhlenbeck, O. C., Martin, F. H., & Doty, P. (1971) *J. Mol. Biol. 57*, 217-229.
Wallace, R. B., Shaffer, J., Murphy, R. F., Bonner, J., Hirose, T., & Itakura, K. (1979) *Nucleic Acids Res. 6*, 3543-3557.
Young, P. R., & Kallenbach, N. R. (1978) *J. Mol. Biol. 126*, 467-479.

Structure and Energetics of a Hexanucleotide Duplex with Stacked Trinucleotide Ends Formed by the Sequence d(GAATTCGCG)†

Dinshaw J. Patel,* Sharon A. Kozlowski, Luis A. Marky, Janet A. Rice, Chris Broka, Keiichi Itakura, and Kenneth J. Breslauer

ABSTRACT: Nuclear magnetic resonance (NMR) and differential scanning calorimetry (DSC) have been used to investigate structural and energetic features of the helix-to-coil transition of the duplex formed by the partially self-complementary sequence d(GAATTCGCG) (henceforth called 9-mer). These results are compared with those obtained from a corresponding study on the helix-to-coil transition of the duplex formed by the fully self-complementary sequence d-(GGAATTCC) (henceforth called 8-mer). The two sequences contain a common GAATTC hexanucleotide duplex with this core flanked by d(GCG) trinucleotide ends in the 9-mer and by dG·dC base pairs in the 8-mer duplex. The NMR parameters for the 9-mer reveal formation of the hexanucleotide core duplex and stacking of the unpaired bases at the trinucleotide ends. The imino proton line widths suggest that under the conditions of the NMR experiment and at low temperature the 9-mer duplexes aggregate through pairing of the complementary ends. DSC on both the 8-mer and 9-mer duplex in 1 M NaCl reveals that the calorimetric transition enthalpies are essentially equal [~60 kcal (mol of double strand)$^{-1}$] despite a 6.2 °C higher melting temperature, T_m, for the 8-mer relative to the 9-mer duplex. From a comparison of the model-dependent van't Hoff and model-independent calorimetric enthalpies we conclude that the helix-to-coil transition of the 8-mer approaches two-state behavior while the corresponding 9-mer transition involves intermediate states. We assign the cooperative component of the 9-mer transition to disruption of the hexanucleotide duplex core with the remaining noncooperative component being associated with the disruption of the stacked ends.

The early research on the helix-coil transition of DNA and RNA oligonucleotide sequences focused on fully base-paired duplexes (Cross & Crothers, 1971; Patel, 1974; Breslauer et al., 1975; Borer et al., 1975; Kallenbach et al., 1976; Breslauer & Sturtevant, 1977; Early et al., 1977, 1980; Patel & Canuel, 1979; Miller et al., 1980; Pardi et al., 1981; Albergo et al., 1981; Marky et al., 1981; Patel et al., 1981a). More recent efforts have extended these investigations to oligonucleotides containing mismatched base pairs and extra bases on one of the strands in the interior of duplex regions (Haasnoot et al., 1980; Cornelis et al., 1979; Patel et al., 1981b,c).

By contrast, there is limited information on the structure and energetics of oligonucleotide duplexes containing single-stranded ends (Uhlenbeck et al., 1973; Romaniuk et al., 1978; Alkema et al., 1981). We report here a nuclear magnetic

†From Bell Laboratories, Inc., Murray Hill, New Jersey 07974 (D.J.P., S.A.K., and J.A.R.), the Department of Chemistry, Douglass College, Rutgers University, New Brunswick, New Jersey 08854 (L.A.M. and K.J.B.), and the City of Hope National Medical Center, Duarte, California 91010 (C.B. and K.I.). *Received May 22, 1981; revised manuscript received September 3, 1981.* K.J.B. and L.A.M. gratefully acknowedge support from the National Institues of Health, Grant GM-23509, the Research Corporation, and the Charles and Johanna Busch Memorial Fund.

0006-2960/82/0421-0451$01.25/0 © 1982 American Chemical Society